



## OPEN

# ZNF32 inhibits autophagy through the mTOR pathway and protects MCF-7 cells from stimulus-induced cell death

SUBJECT AREAS:  
MACROAUTOPHAGY  
BREAST CANCER

Received  
16 September 2014

Accepted  
24 February 2015

Published  
19 March 2015

Correspondence and  
requests for materials  
should be addressed to  
P.L. (linping8@yahoo.  
com)

Yanyan Li<sup>1</sup>, Le Zhang<sup>1</sup>, Kai Li<sup>1</sup>, Jun Li<sup>1</sup>, Rong Xiang<sup>2</sup>, Jie Zhang<sup>1</sup>, Hongjiang Li<sup>3</sup>, Yan Xu<sup>4</sup>, Yuyan Wei<sup>1</sup>, Junping Gao<sup>1</sup>, Ping Lin<sup>1</sup> & Yuquan Wei<sup>5</sup>

<sup>1</sup>Division of Experimental Oncology, State Key Laboratory of Biotherapy/Collaborative Innovation Center for Biotherapy, West China Hospital, Sichuan University, Chengdu, China, <sup>2</sup>Department of clinical medicine, School of Medicine/Collaborative Innovation Center for Biotherapy, Nankai University, Tianjin, China, <sup>3</sup>Department of Thyroid and Breast Surgery, West China Hospital, Sichuan University, Chengdu, China, <sup>4</sup>Biorepository, State Key Laboratory of Biotherapy/Collaborative Innovation Center for Biotherapy, West China Hospital, Sichuan University, Chengdu, China, <sup>5</sup>Division of Cancer Biotherapy, State Key Laboratory of Biotherapy/Collaborative Innovation Center for Biotherapy, West China Hospital, Sichuan University, Chengdu, China.

**ZNF32 is a recently identified zinc finger protein and its functions remain largely unknown. Autophagy has been shown to affect cell proliferation and survival. Here, we innovatively show the effect of ZNF32 on cell autophagy and autophagy-associated cell death in breast carcinoma cells and also elucidate its underlying mechanisms. We examined the autophagic activity and LC3 II expression in human carcinoma cell lines with increased or decreased ZNF32 expression. Pharmacological inhibition (rapamycin) or activation (EGF) assays were used to investigate the function of the AKT/mTOR pathway during this process. H<sub>2</sub>O<sub>2</sub>- and diamide-induced MCF-7 cell death models were used to elucidate the role of ZNF32-associated autophagy in breast carcinoma cell death. Our results show that increasing ZNF32 expression in MCF-7 cells inhibits autophagy initiation by activating the AKT/mTOR pathway, and further reduced autophagy-associated cell death and maintained MCF-7 cell survival. Conversely, impairing ZNF32 expression by transfecting ZNF32 siRNA strongly promoted autophagy, further augmenting autophagy-associated cell death. Furthermore, correlations between ZNF32 and autophagy were observed in both MCF-7 xenograft tumors and in breast cancer patients. In conclusion, ZNF32 acts as an effective autophagy inhibitor to protect breast cancer cells from excessive stimulus-autophagy-induced cell death.**

**H**uman Zinc Finger Protein 32 (ZNF32), a recently discovered zinc finger protein, maps to chromosome 10q<sup>23–24</sup>. ZNF32 is reported to be a transcription factor belonging to the Kruppel-related zinc finger family<sup>1</sup>. Based on our previous study, mouse Zinc Finger Protein 637 (ZFP637), the homologous gene of human ZNF32, was implicated in promoting EMT-6 (a mouse breast carcinoma cell line) proliferation<sup>2</sup> and preventing C2C12 (a mouse myoblast cell line) differentiation<sup>3</sup>. However, the exact functions of human ZNF32 remain largely unknown. Potential target genes of ZNF32 remain under investigation. The mechanisms of ZNF32-associated transcription regulation and its downstream events also remain unclear.

Autophagy is generally considered to be a process of cellular self-renewal, including the formation of autophagosomes and the degradation of organelles and cytosolic macromolecules<sup>4</sup>. With the assistance of autophagy-related gene 5–12 (Atg5–Atg12) conjugates, the precursor of microtubule-associated protein 1 light chain 3 alpha (LC3), a homolog protein of the yeast autophagy marker Atg8 and an interactive protein of the microtubule-associated protein 1 (MAP-1) family<sup>5–7</sup>, is cleaved to form cytosolic LC3 I, which further conjugates with phosphatidylethanolamine to produce the isolation membrane-associated LC3 II<sup>8,9</sup>. Dysfunctional organelles or misfolded proteins are escorted into autophagosomes for lysosomal degradation after binding to a substrate receptor<sup>10,11</sup>. However, excessive autophagic activity has been shown to result in cell death, which has been designated as type II programmed cell death or autophagy-associated cell death. In other words, basal autophagy has been shown to barely affect cell death, but the excessive autophagy induced by intense stimuli usually results in cell damage or even cell death. In recent years, increasing evidence has suggested that the autophagy of cancer cells is involved in cancer growth and progression<sup>12</sup>. Indeed, autophagy, a double-edged sword, has been reported to differentially influence cancer cell fate in different cell types and under different stimulus intensities<sup>13–15</sup>. On the one hand, autophagy can protect cancer cells from unfavorable growth condition and further attenuate the



efficiency of anticancer drugs<sup>16</sup>. On the other hand, some reports have indicated that autophagy-associated cell death decreases cancer cell viability and enhances chemotherapy-associated anticancer activity<sup>17,18</sup>.

The formation of an autophagosome has been conventionally regarded as the initial step of autophagy. Currently, two major signaling pathways have been shown to be involved in this process<sup>19</sup>. In mammalian cells, autophagy initiation can be induced via the phosphoinositide 3-kinase/Protein Kinase B/mammalian target of rapamycin (PI3K/AKT/mTOR) pathway<sup>20</sup>. Moreover, nutrients have also been shown to regulate the initiation of autophagy through the serine/threonine kinase 11 (STK11, LKB1)/AMP-activated protein kinase (AMPK)/mTOR pathway<sup>21,22</sup>. Conversely, the B-cell CLL/lymphoma 2 (Bcl-2) family, which are anti-apoptotic proteins, exerts an opposite effect on autophagy initiation via two different pathways. First, Bcl-2 can prevent Beclin-1 from binding to PI3KCIII (class III PI3K) and then inhibit autophagy initiation through the PI3K/AKT/mTOR pathway<sup>20,23</sup>. Second, the Bcl-2 family can inhibit Beclin-1 function, which elevates p27 and Atg5 expression and facilitate autophagy through the LKB1/AMPK/mTOR pathway<sup>21,22</sup>.

Autophagy is closely related to cancer survival<sup>24</sup>. It remains unknown whether human ZNF32 modulates autophagic activity in carcinoma cells and affects cell viability. The underlying mechanisms of ZNF32-associated autophagy also remain unknown. Breast cancer causes high morbidity in women. Consequently, we aimed to investigate the effect of ZNF32 on breast cancer autophagy and viability and elucidate the underlying molecular mechanisms. Furthermore, we also analyzed the correlations between ZNF32 and autophagy in both xenograft tumors and in breast carcinoma patients.

## Results

**ZNF32 reduces autophagosome formation and inhibits autophagy initiation in MCF-7 cells.** To investigate the effect of ZNF32 on autophagy in breast cancer cells, ZNF32 siRNA and expression plasmids were introduced into a human breast carcinoma cell line (MCF-7). Acidic vesicular organelles (AVO) were visualized using AO staining (details described in Materials and methods). Strikingly, increasing ZNF32 expression in MCF-7 cells significantly reduced the percentage of AVO-positive cells. By contrast, interfering with ZNF32 expression increased the mean AVO-positive cell number (Fig. 1A). Additionally, we evaluated LC3 to further verify autophagosome formation. Plasmids expressing red fluorescent protein RFP-LC3-fusion protein were transfected into cells to label cytoplasmic autophagosomes<sup>25</sup>. Consistent with the previous result, a reduction in positive cells with punctiform aggregates was observed in the ZNF32-overexpressing cells, whereas more positive cells with punctiform aggregates were observed in ZNF32 knockdown cells (Fig. 1B). Moreover, a western blot analysis further verified that the expression of LC3 II, the lipidated form of LC3 associated with the autophagosomal membrane, decreased after ZNF32 overexpression. Conversely, LC3 II expression was higher in ZNF32-deficient cells (Fig. 1C). The same phenomenon was also observed in other breast cancer cell lines, such as SK-BR-3 and MDA-MB-231 (Fig. S1). In conclusion, these findings indicate that ZNF32 effectively decreases the autophagosome number and influences the autophagic process in breast carcinoma cells.

The quantity of autophagosomes is mainly determined by two independent processes of autophagy, which are autophagosome formation and autophagosome-lysosome fusion for subsequent degradation. Consequently, we examined which process was directly involved in ZNF32-associated regulation. To identify the precise process, NH<sub>4</sub>Cl was used to block autophagosome-lysosome fusion and autophagolysosome degradation<sup>26</sup>. Surprisingly, preventing the degradation of autophagosome adequately restored the number of AVO-positive cells (Fig. 1D) and the LC3 II level (Fig. 1E) in both the ZNF32-deficient and overexpressing cells. These results show that

ZNF32 suppresses autophagy initiation whether autophagosome-lysosome fusion is allowed.

**ZNF32 inhibits autophagy initiation by activating the AKT/mTOR pathway.** ZNF32 has been shown to be involved in the initial step of autophagy. However, the underlying signaling pathway through which this generally accepted transcription factor regulates autophagosome formation required further investigation. Two classic signaling pathways have been implicated in mediating the initiation of autophagy: the Beclin-1-dependent p27/Atg5 and Beclin-1-dependent AKT/mTOR pathways. Beclin-1 has been reported to participate in both pathways. To investigate the mechanism in which ZNF32 affects autophagy, we first examined the expression of Beclin-1 in MCF-7 cells with modified ZNF32 expression. Similar to autophagy initiation, Beclin-1 expression was significantly suppressed in ZNF32-overexpressing cells and was increased in ZNF32-deficient cells (Fig. 2A). To further clarify which downstream pathway might be involved, we examined the expression of the key molecules in the both pathways. We found that although the expression levels of Beclin-1 and Atg5 were increased in the ZNF32-deficient MCF-7 cells, the expression level of p27 remained unchanged (Fig. 2A). This finding suggests that the p27-associated pathway is not involved in ZNF32-associated autophagy.

The Beclin-1-dependent AKT/mTOR pathway is another mediator of autophagy initiation. To determine whether this pathway is involved in ZNF32-regulated autophagy, the activation of AKT and mTOR was evaluated after increasing or decreasing ZNF32 expression in MCF-7 cells. Interestingly, increasing ZNF32 expression clearly promoted the phosphorylation of both AKT and mTOR (Fig. 2A). It is widely accepted that the AKT/mTOR pathway inhibits autophagy initiation. Therefore, it was hypothesized that an increase in ZNF32 can induce AKT/mTOR activation, which would further interfere with autophagy initiation. To test this hypothesis, rapamycin (rapa), a classic mTOR inhibitor<sup>27</sup>, was used to investigate the effect of mTOR on ZNF32-associated autophagy. Consistent with our hypothesis, inhibiting mTOR activation rescued ZNF32-induced autophagy deficiency (Fig. 2B, D). Furthermore, the EGF activation of the AKT/mTOR pathway reduced LC3 II production and inhibited autophagosome formation in ZNF32-deficient MCF-7 cells (Fig. 2C, D). Additionally, we also rescued ZNF32 expression in the ZNF32-knockdown MCF-7 cells to further verify its function in autophagy (Fig. 2E). These results demonstrate that ZNF32 can activate the AKT/mTOR pathway, suppressing autophagy initiation.

**ZNF32-associated autophagy participates in H<sub>2</sub>O<sub>2</sub>- and diamide-induced cell death.** Although closely associated with autophagy, ZNF32 has demonstrated no effects on cell viability without stimulation (Fig. 3A, D control group). Autophagy has been reported to mediate stimulus-induced cell death<sup>28</sup>. First, to verify the effect of autophagy on H<sub>2</sub>O<sub>2</sub>- and diamide-induced cell death, high doses of H<sub>2</sub>O<sub>2</sub> (700 μmol/L) and diamide (500 μmol/L) were used. A MTT assay was used to evaluate cell death (Fig. 3A). The results showed that a ZNF32 deficiency augmented this stimulus-induced cell death. Indeed, with H<sub>2</sub>O<sub>2</sub> or diamide stimulation, the LC3 II expression level increased in both si-NC and ZNF32 knockdown cells, but the increases appeared to be more dramatic in the ZNF32 knockdown cells (Fig. 3B). Consequently, we proposed that ZNF32-regulated autophagic activity could further affect H<sub>2</sub>O<sub>2</sub>- and diamide-induced cell death. To test this proposal, we first examined the autophagic activity in ZNF32-modified MCF-7 cells treated with H<sub>2</sub>O<sub>2</sub> and diamide. Consistent with our previous observation, ZNF32-knockdown MCF-7 cells demonstrated the highest level of autophagic activity after stimulation with H<sub>2</sub>O<sub>2</sub> and diamide (Fig. 3C). Moreover, Wor, which is a specific inhibitor of autophagy that has been shown to diminish spontaneous autophagy (Fig. 3C the upper two of the 2<sup>nd</sup> vertical row), also reduced stimulus-triggered autophagy (Fig. 3C the 3<sup>rd</sup> vertical row); the bar results are

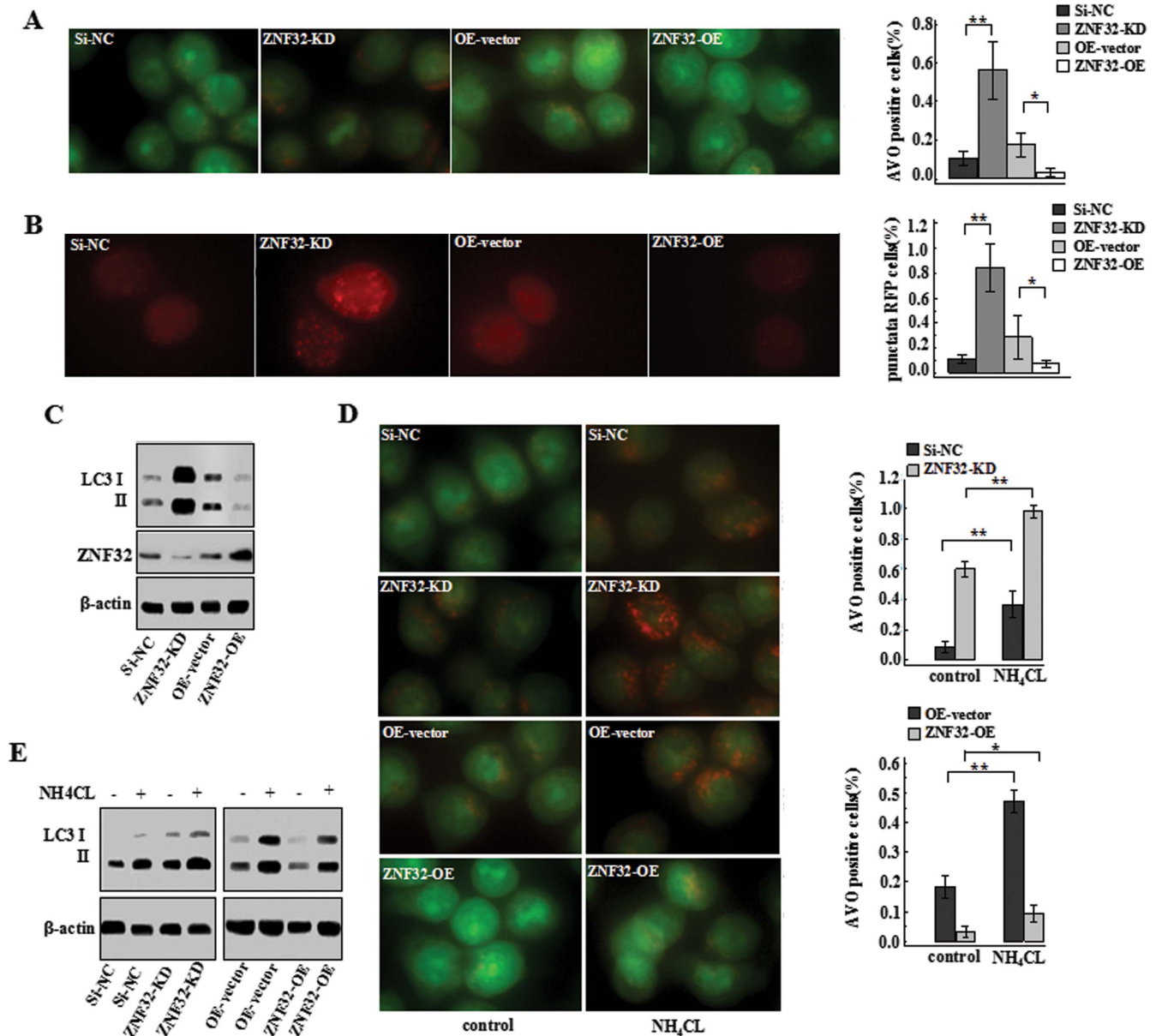


**Figure 1 | ZNF32 reduces autophagosome formation and inhibits autophagy initiation in MCF-7 cells with ZNF32 knock down (ZNF32-KD) or overexpression (ZNF32-OE).** (A) Images of acridine orange (AO) staining and (B) RFP-LC3 transfection in cells as detected using fluorescence microscopy are shown. (C) LC3 II expression levels were measured using western blot analysis. (D) AO staining and (E) LC3 II expression in cells treated with 20 mmol/L NH<sub>4</sub>CL for 24 h.  $\beta$ -actin was used as a loading control. The full size blots were shown in the Supplementary Figure S4 and band of interest is indicated with an arrow.

shown on the right. Interestingly, as shown in Fig. 3D and E, Wor partially reduced the H<sub>2</sub>O<sub>2</sub>- and diamide-induced cell death in these cells and reduced the difference between the ZNF32-knockdown and corresponding control cells (Fig. 3D the 3<sup>rd</sup> vertical row). Atg5 is thought to be an essential gene for autophagy<sup>29,30</sup> and has been shown to be involved in the formation of autophagosome<sup>31</sup>. Because of the controversial role of Wor and considering its unrelated side effects, Atg5 siRNA was used. Silencing Atg5 clearly decreased LC3 II expression (Fig. 3F) and also reduced the difference in H<sub>2</sub>O<sub>2</sub>- and diamide-induced viability between the ZNF32-knockdown and corresponding control cells (Fig. 3G). Overall, these results indicate that ZNF32-associated autophagy facilitates stimulus-induced cell death to some extent.

**AKT/mTOR pathway is involved in the ZNF32-autophagy-cell death axis.** The AKT/mTOR pathway has been shown to be

involved in ZNF32-associated autophagy, which may affect stimulus-induced cell death. Therefore, we intended to further verify that the AKT/mTOR pathway participates in the ZNF32-autophagy-cell death axis. Strikingly, in ZNF32-overexpressing MCF-7 cells, inhibiting mTOR activation with rapa partially rescued the autophagic activity (Fig. 2B and Fig. 2D) and slightly increased H<sub>2</sub>O<sub>2</sub>- and diamide-induced cell death (Fig. 4A and B). Moreover, EGF was also used to activate the AKT/mTOR signaling pathway in ZNF32-deficient MCF-7 cells. Similarly, activation of the AKT/mTOR pathway inhibited autophagy and partially counteracted the ZNF32-enhanced cell death after H<sub>2</sub>O<sub>2</sub> and diamide treatment (Fig. S2). These findings suggest that ZNF32 inhibits stimulus-induced autophagy and cell death at least partially through AKT/mTOR activation.

**ZNF32 is correlated with autophagy in both xenograft tumor-loaded mice and in breast cancer patients.** To investigate the

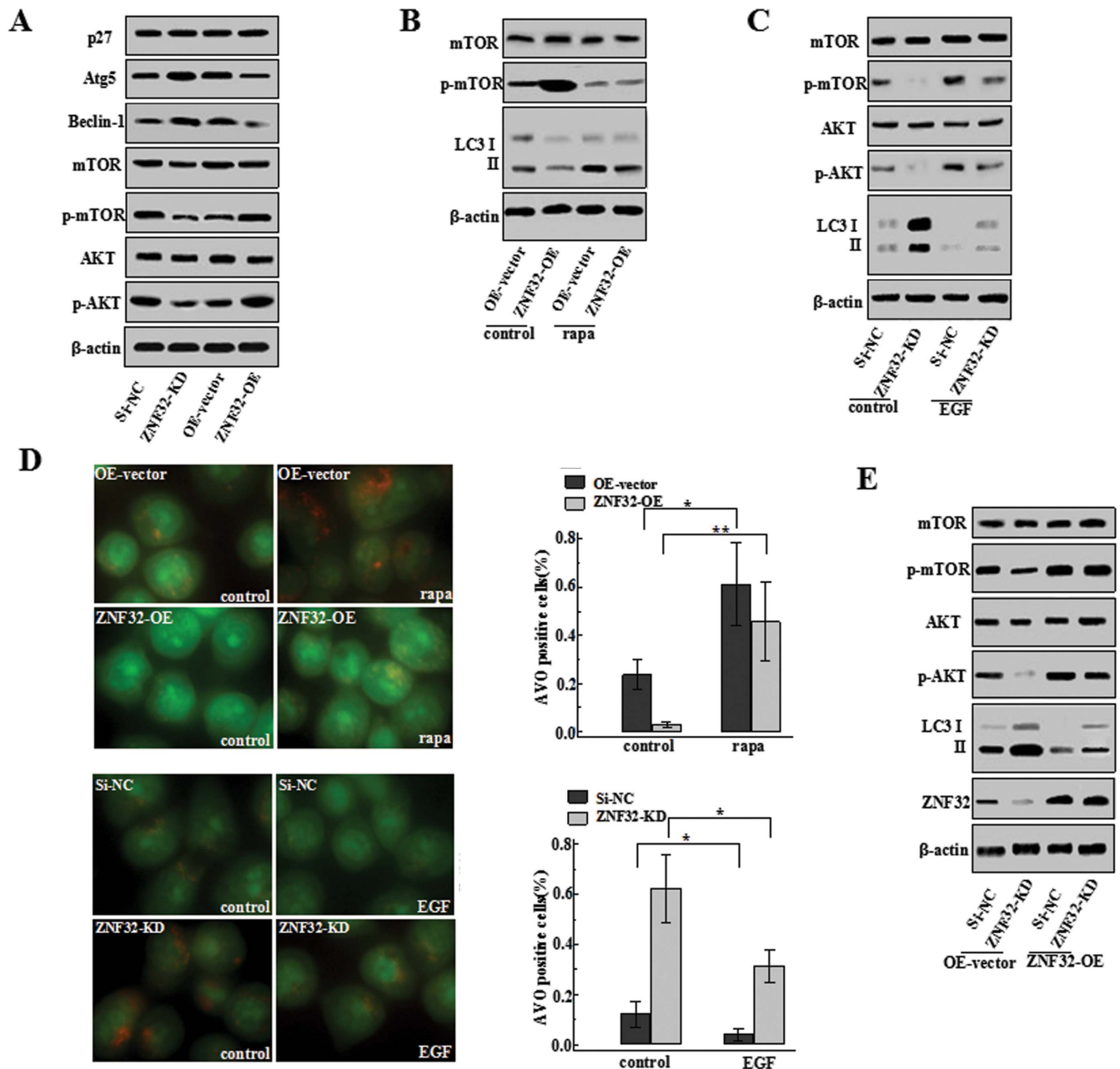


**Figure 2** | ZNF32 inhibits autophagy initiation by activating the AKT/mTOR pathway. (A) Effects of ZNF32-KD or ZNF32-OE on p27, Atg5, Beclin-1, p-AKT and p-mTOR expression. (B) mTOR activation in MCF-7 cells with ZNF32 overexpression after a 24 h treatment with 100 nmol/L rapa was determined using western blot analysis. (C) Phosphorylation of mTOR and AKT in MCF-7 cells with ZNF32 overexpression or knockdown after a 24 h treatment with 1 ng/ml EGF. (D) AO staining in MCF-7 ZNF32-KD or ZNF32-OE cells after 24 h treatment with 100 nmol/L rapa or 1 ng/ml EGF was detected using fluorescence microscopy. (E) ZNF32 expression rescues AKT/mTOR activation and LC3 II expression in ZNF32 knockdown cells.  $\beta$ -actin was used as a loading control. The full size blots were shown in the Supplementary Figure S5 and band of interest is indicated with an arrow.

impact of ZNF32 on autophagy in vivo, a MCF-7-bearing mouse model was constructed. Interestingly, although unable to directly affect cell viability in vitro, ZNF32 was observed to regulate tumor growth in vivo (Fig. 5A). Surprisingly, inconsistent with our prediction, we found that ZNF32 knockdown of MCF-7 cells could form tumor masses that were larger in volume and weight in the null mouse models (Fig. 5B, C). Next, we examined the autophagic status of the xenograft tumors. Consistent with the previous in vitro results, decreasing ZNF32 expression also promoted autophagy in the xenograft tumors. As shown in Figure 5D, LC3 II expression was higher in the ZNF32-deficient tumors. Additionally, AKT/mTOR activation was inhibited after interfering with ZNF32 expression.

Moreover, the p27 pathway appeared to remain unchanged (Fig. 5D). These results imply that ZNF32 also modulates autophagic activity via the AKT/mTOR pathway in vivo. However, its impact on tumor growth is complicated.

To better understand the relationship between ZNF32 and autophagy, we collected breast cancer samples from 49 cases and used western blot analysis to detect the ZNF32 and LC3 II expression levels. Based on the ZNF32 and LC3 II expression levels, we conducted a correlation analysis (Fig. 5E). Surprisingly, we found that ZNF32 expression was positively correlated with LC3 II expression in breast cancer patients ( $R = 0.807$ ). Considering that MCF-7 is a luminal A subtype (ER and PR positive, Her-2 negative) cell line

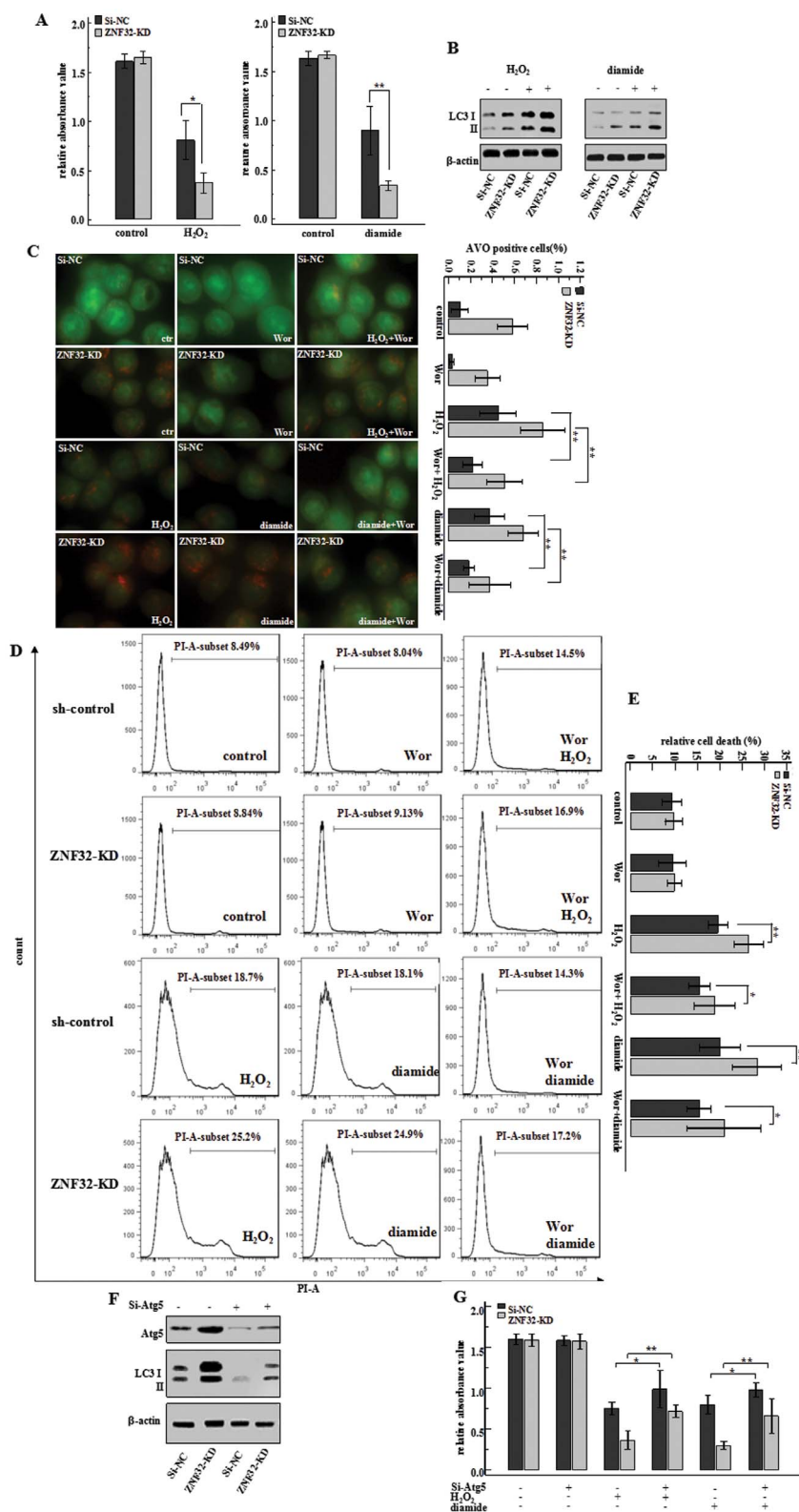


**Figure 3** | ZNF32-associated autophagy participates in  $H_2O_2$ - and diamide-induced cell death. (A) MTT assay showing the effect of ZNF32 on cell viability after 24 h treatment with  $H_2O_2$  (700  $\mu\text{mol/L}$ ) or diamide (500  $\mu\text{mol/L}$ ). (B) LC3 II expression after a 24 h treatment with  $H_2O_2$  or diamide in ZNF32-KD cells. (C) Images of AO staining in ZNF32-KD cells after a 24 h treatment with  $H_2O_2$  or diamide with a 3 h pre-treatment with or without Wor (100 nmol/L). Wor has been shown to diminish spontaneous autophagy (the upper two of the 2<sup>nd</sup> vertical row) and reduced stimulus-triggered autophagy (the 3<sup>rd</sup> vertical row). (D) Flow cytometry assay showing the effect of ZNF32-KD on cell death after a 24 h treatment with  $H_2O_2$  or diamide with a 3 h pre-treatment with or without Wor (100 nmol/L). (E) The bar results are shown. (F) Atg5 interference efficiency and LC3II expression were detected using western blot analysis.  $\beta$ -actin was used as a loading control. The full size blots were shown in the Supplementary Figure S6 and band of interest is indicated with an arrow. (G) MTT assay showing the effect of si-Atg5 on MCF-7 cell viability after a 24 h treatment with  $H_2O_2$  or diamide.

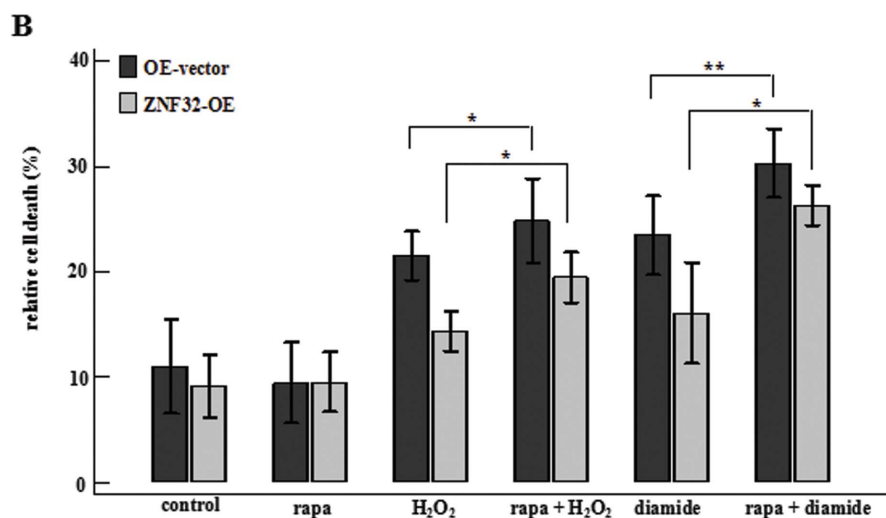
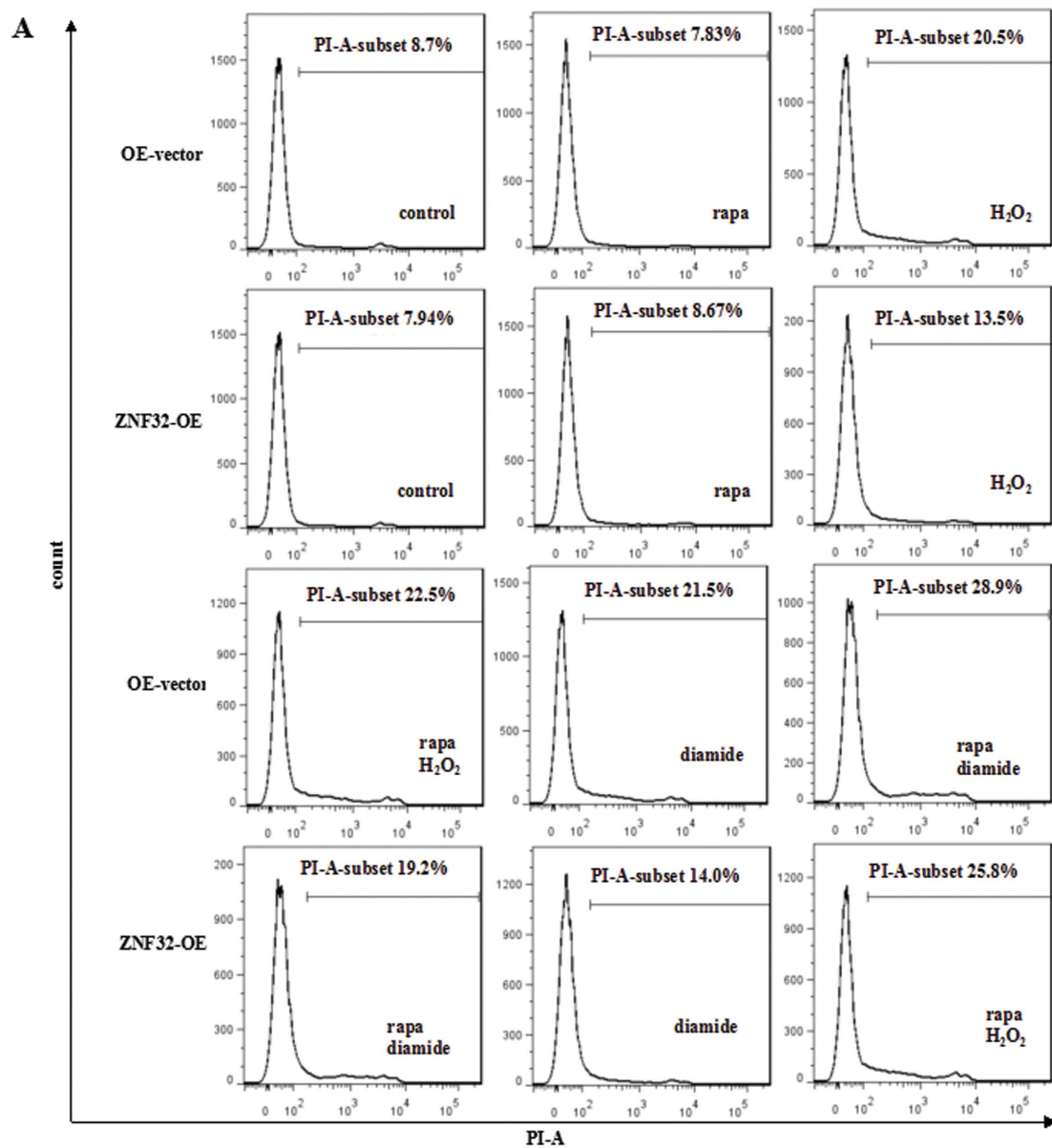


**Figure 4** | AKT/mTOR pathway is involved in the ZNF32-autophagy-cell death axis. (A) Flow cytometry reveals the effect of ZNF32 knockdown on cell death after a 24 h treatment with H<sub>2</sub>O<sub>2</sub> (700 μmol/L) or diamide (500 μmol/L). rapa (100 nmol/L) was used to inhibit mTOR activation in a 3 h pre-treatment before added H<sub>2</sub>O<sub>2</sub> or diamide. (B) The bar results are shown.



and that the luminal subtype is common, we divided these samples into 23 cases of luminal A subtype, 20 cases of luminal B subtype (ER and PR positive, Her-2 positive) and 4 Her-2-enrich cases, 1 basal-like case, 2 normal-like cases, based on the intrinsic molecular subtypes of breast cancer<sup>32–34</sup>. Consistent with the trends observed in the 49 cases overall, we found that ZNF32 expression was positively correlated with LC3 II expression in both subtypes of breast cancer samples (Fig. 5F luminal A subtype and Fig. 5G luminal B phenotype). The sample sizes of the other group cases were too small to conduct a correlation analysis. Somehow, this result seems to contradict the observations made *in vitro* and in the mouse models. These findings suggest that more complicated factors may also be involved in the ZNF32-associated regulation of autophagy in cancer patients. Furthermore, we compared the ZNF32 and LC3 II expression levels in two groups of patients with high and low pathological grades of breast cancer (see details in Materials and methods, Elston-Ellis modification of the Scarff-Bloom-Richardson Grading System). However, there were no significant differences in the ZNF32 and LC3 II expression levels between these two pathological grade groups (Fig. 5H), even in the luminal A and luminal B subtype breast cancer samples (Fig. S3). We also compared the ZNF32 and LC3 II expression levels in the luminal A and luminal B subtype breast cancer samples (Fig. 5I). There were no significant differences in the ZNF32 and LC3 II expression levels between the two groups, suggesting that the trend in ZNF32 and LC3 II expression may be irrelevant to the gene expression-based “intrinsic” subtype. Although there was no significant difference between the two pathological grade groups, possibly because of the small sample size or other unknown factors, we observed an accelerated growth of ZNF32-deficient breast cancer cells in the mouse models. The relationship between ZNF32 and the pathological grade of breast cancer may be quite complicated inside organisms. However, it was shown that the ZNF32 and LC3 II expression levels are correlated in breast carcinoma patients.

## Discussion

Currently, resistance to general therapies, including chemotherapy, radiotherapy and immunotherapy, perplexes oncologists and clinicians worldwide. How to overcome this obstacle is a wide concern. Clarifying the underlying mechanisms may greatly improve the efficiency of cancer therapies. Recently, autophagy has been shown to contribute to the therapy-associated resistance of cancer<sup>35</sup>. However, the exact role of cancer cell autophagy in resistance to treatment is still controversial. ZNF32, a recently discovered transcription factor, has been shown to be closely associated with oxidative stress. In this study, we elucidated a novel function of ZNF32 in autophagy and autophagy-associated cell death. ZNF32 was shown to activate the AKT/mTOR pathway, which subsequently decreases the severe autophagic activity in breast carcinoma cells. ZNF32 may protect breast cancer cells from excessive autophagy-associated cell death. Moreover, ZNF32 was also shown to be correlated with autophagy in xenograft tumor-loaded mice and cancer patients. Altogether, we indicate that ZNF32 may be a potential target for breast cancer treatment.

We found that ZNF32 inhibited the initiation of autophagy by activating the AKT/mTOR pathway. However, as a transcription factor and not a phosphokinase, ZNF32 cannot directly phosphorylate AKT/mTOR. There must be an unknown intrinsic link between ZNF32 and AKT/mTOR activation. The direct target genes of ZNF32 involved in AKT/mTOR activation still remain unknown. According to bioinformatics data, there may be a potential ZNF32 binding sequence in the PI3K promoter region. Perhaps, ZNF32 directly induces PI3K expression and activates AKT/mTOR. A further investigation is required to answer this question.

Based on our observations, even though interfering with ZNF32 expression augmented spontaneous autophagy in carcinoma cells,

the viability of these cells remained unaffected. This finding suggests that the level of ZNF32-induced autophagy was lower than the autophagic threshold that induces cell death. Reactive oxygen species (ROS) have been widely recognized to mediate cancer development and progression. Indeed, H<sub>2</sub>O<sub>2</sub> and diamide, the conventional ROS inducers, adequately promoted autophagy, decreasing the viability of cancer cells. In this case, ZNF32 prevented the excessive autophagic activity induced by ROS, reducing cell death. In ZNF32-defective carcinoma cells, which lack this protective mechanism, ROS may induce a higher level of autophagy and increase cancer cell death. It has been reported that the zinc-finger protein MCPIP-induced ROS causes an ER stress response, inducing autophagy<sup>36</sup>. Our data (unpublished) indicated that ZNF32 may affect the function of mitochondria. The change in mitochondria function may be one of the factors affecting autophagy. Perhaps ZNF32 also functions in organelles, such as the mitochondria or ER, to regulate autophagy. Whether ZNF32-associated autophagy affects cell death induced by factors other than ROS warrants additional investigation.

Although ZNF32 appears to reduce autophagy and increase cell viability *in vitro*, decreasing ZNF32 expression in xenograft tumors increased the mean volume and weight of the tumors *in vivo*. More interestingly, consistent with the *in vitro* results, the autophagic activity in the ZNF32-knockdown xenograft tumors appeared to be elevated according to the LC3 II expression pattern. Most unpredictably, we observed a positive correlation between ZNF32 and autophagy in breast cancer patients, which was inconsistent with our observations *in vitro* and in the mouse models. An analysis of the pathological grades of the breast cancer patient revealed that there was no difference in the ZNF32 and LC3 II expression levels, even between the luminal A and luminal B subtypes. Indeed, multiple factors, besides autophagy, may contribute to tumor growth *in vivo*. Some studies have reported that autophagy can promote cell death and make tumor cells more sensitive to stimulation<sup>37</sup>. Some studies, however, have reported different points of view<sup>13,38</sup>. Although we cannot attribute all the differences of tumor growth to autophagy, it may affect tumor growth to some extent as autophagy appears to be involved in tumorigenesis, cancer development and treatment outcome<sup>39,40</sup>. Because of the advances in cancer research, autophagy may act as a cancer suppressor or promoter depending on the different cell types, grades and therapeutic strategies<sup>40,41</sup>. Studies have reported that autophagy can promote or prevent apoptosis in the same cell type; the response is governed by the nature of the death stimulus and the compensatory changes in other forms of autophagy<sup>28,42</sup>. ZNF32 may regulate autophagy under more control *in vivo*. The diversity of the tumor microenvironment complicates the analysis of the *in vivo* mechanisms underlying ZNF32 regulation of tumor growth. Perhaps this diversity is why our *in vitro*, *in vivo* and patient sample results were not consistent. Explaining this inconsistency requires further investigation. We are further studying the complexity of ZNF32 regulation of tumor growth *in vivo*. All of the results indicated that ZNF32 is associated with breast cancer autophagy. We believe that ZNF32-associated gene therapy may improve the therapeutic efficiency of chemotherapy and benefit cancer patients. Until recently, several lines of evidence have indicated that ZNF32 may be involved in the diverse processes of cancer progression. Consequently, we faithfully recognize that a further investigation of ZNF32 functions in cancer biology would stimulate great advances in cancer diagnostics and therapeutics.

## Methods

**Cells, reagents and antibodies.** The MCF-7, SK-BR-3 and MDA-MB-231 cell lines were maintained in complete Dulbecco's modified Eagle's medium (DMEM) and RPMI 1640 medium containing 10% FBS in humidified atmosphere at 37°C, 5% CO<sub>2</sub>. Wortmannin (Wor), NH<sub>4</sub>Cl, H<sub>2</sub>O<sub>2</sub>, rapamycin (rapa), diamide, epidermal growth factor (EGF) were purchased from Sigma-Aldrich (St Louis, MO, USA). The Cell Apoptosis Assays Kit was purchased from Kaiji (Nanjing, China).

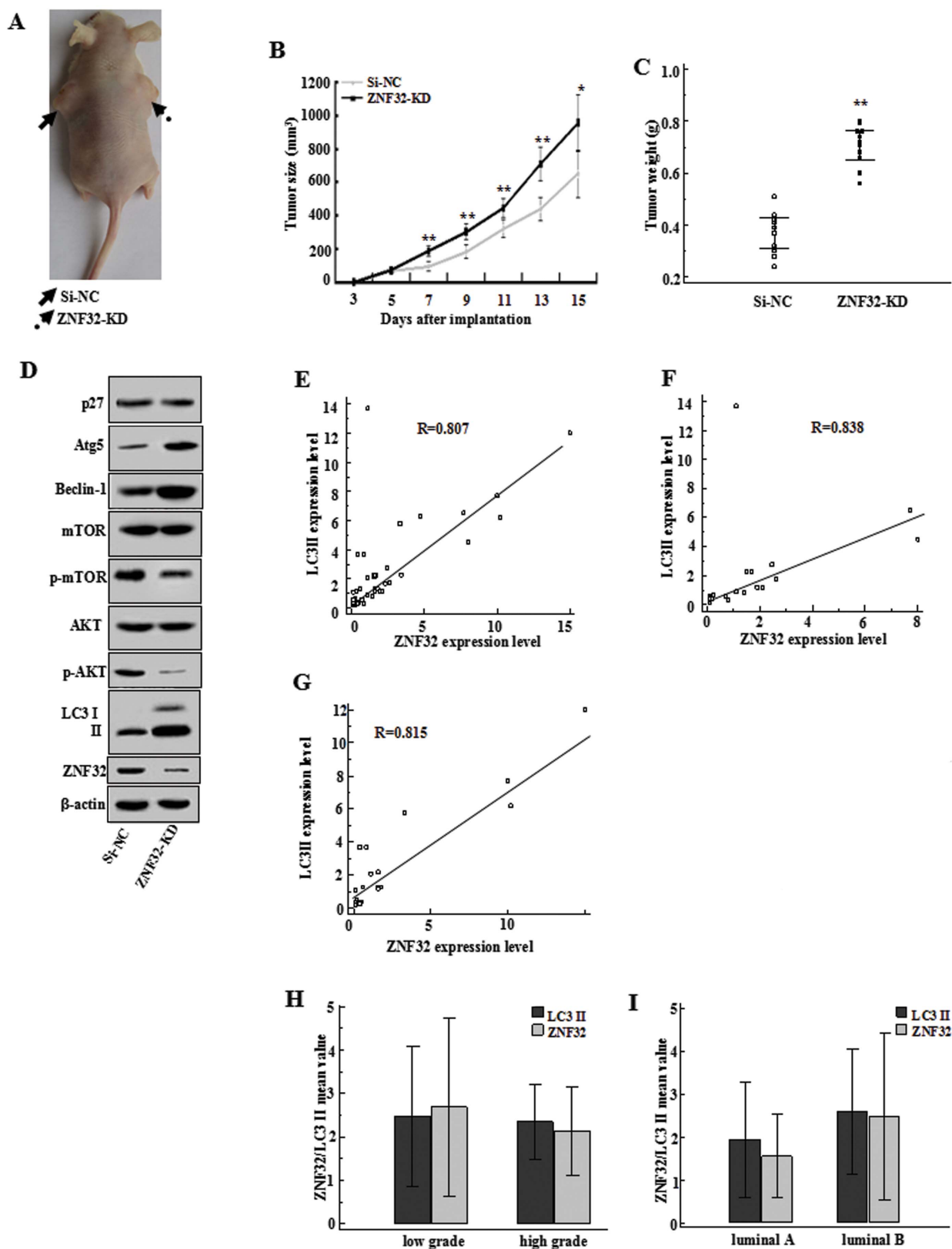


**Figure 5** | ZNF32 is correlated with autophagy in both xenograft tumor-loaded mice and in breast cancer patients. (A) A total of  $5 \times 10^6$  viable MCF-7 si-NC or ZNF-32 KD cells were implanted subcutaneously into nude mice. Pictures of the treatment group are shown. Mice were killed 2 weeks after implantation. (B) Tumor growth (volume) from the 3<sup>rd</sup> to 15<sup>th</sup> day after implantation. (C) Tumor weight (g) was measured on the 15th day after implantation. (D) Western blot results showing the expression levels of some autophagy related markers in tumor tissues.  $\beta$ -actin was used as a loading control. The full size blots were shown in the Supplementary Figure S6 and band of interest is indicated with an arrow. Correlation analysis between ZNF32 and LC3 II in (E) the total (F) luminal A subtype and (G) luminal B subtype breast cancer patient samples. Expressions of ZNF32 and LC-3 II in (H) low or high pathological grade (I) luminal A or luminal B subtype of breast cancer samples.





**Western blot analysis.** Protein from cells or tissue samples was extracted using General Protein Extraction Reagent (Biotek, Beijing, China) supplemented with 1% protease inhibitor. A total of 25 µg protein was loaded and separated on 12% SDS-PAGE and then transferred by electrophoresis to 0.45 µm polyvinylidene difluoride membranes. The following antibodies were used: LC3, Atg5, p27, mTOR, phosphorylated mTOR (p-mTOR), AKT, and phosphorylated AKT (p-AKT), which were purchased from Cell Signaling Technology (CST, Danvers, MA, USA). β-actin antibody was purchased from ZhongShanJinQiao (Beijing, China). All of the above-mentioned antibodies were used at a dilution ratio of 1:1000. ZNF32 antibody was produced and purified as previously described<sup>43</sup> and used at a dilution of 1:50. The membrane was developed using Immobilon™ Western Chemiluminescent HRP Substrate (Millipore). Protein levels were quantified using scanning blots on a Gel Doc EZ imager (Bio-Rad, California, USA) and analyzing with Quantity One 1D image analysis software 4.4.0 (Bio-Rad, California, USA).

**Cell viability assay.** Cells were plated onto 96-well plates and treated with H<sub>2</sub>O<sub>2</sub> (700 µmol/L) or diamide (500 µmol/L) or the corresponding solvent control. Cell viability was measured using a MTT assay. The optical density was determined at 570 nm with a reference filter of 630 nm using an ELISA plate reader (Model 550; Bio-Rad). At least three independent experiments were conducted.

**Analysis of cell death.** Cell death was evaluated using a propidium iodide (PI) staining Flow Cytometry analysis Kit (Kaiji, Nanjing, China) according to the manufacturer's instruction. The analysis was performed using a BD FACS Aria (Franklin Lakes, NJ, USA). Individual fluorescent populations were determined using acquisition and analysis software (FlowJo 7.6). Triplicate independent experiments were conducted.

**Transfection.** The pSG5-ZNF32 over-expression plasmid was constructed by inserting expanded ZNF32 cDNA (NCBI Reference Sequence: NM\_006973.2) fragments into pSG5 vectors stored in our lab. RFP-LC3 was stored in our lab. ZNF32, Atg5 and non-target siRNA were purchased from Genepharma (Shanghai, China), ZNF32 siRNA: GUCAGAAAGGAAGCUAAUUTT (sense 5'-3'), Atg5 siRNA: AUCCCAUCCAGUUGCUUGAUC (sense 5'-3'), non-target siRNA: UUCUUCGAAACGUGUCACGUTT (sense 5'-3'). Transfections were mediated by TurboFect Transfection Reagent (Thermo Fisher Scientific, Waltham, MA). Cells were pre-cultured in serum-free DMEM for 2 h before transfection. Then, 6 µg plasmid or 10 nmol siRNA was introduced into the cell using 6 µl transfection reagent according to the manufacturer's instructions. The punctiform aggregates and cells were counted at a final magnification of 400×. The percentage of positive cells with at least 5 punctiform aggregates was calculated; at least 600 cells were observed.

**Acridine orange (AO) staining.** Acridine orange with membrane permeability spontaneously aggregated in acidic autophagosomes and exhibited punctate staining. It is conventionally used to visualize cytoplasmic autophagosome and detect autophagosome formation. To examine the formation of autophagosomes, cells were plated onto 48-well plates at a density of 3 × 10<sup>4</sup> cells per well. Approximately 24 h later, the cells were rinsed with PBS three times. Then, the cells were treated with 1 µg/ml AO at 37°C for 30 min and rinsed with PBS three times. The formation of autophagosomes was observed and images were captured using an inverted fluorescent microscope (Nikon ECLIPSE TE 2000-U). The AO staining punctiform aggregates and the cells were counted at a final magnification of 400×. The percentage of AVO positive cells with at least 10 AVO aggregations was calculated; at least 600 cells were observed. Subsequently, a statistical analysis was performed. Triplicate independent experiments were conducted.

**Animals.** BALB/c male nude mice were used at aged 6–8 weeks. A total of 5 × 10<sup>6</sup> viable MCF-7 cells with low (ZNF32-KD) or normal (si-NC) ZNF32 expression were subcutaneously injected into the lateral backsides of the mouse. The tumor volume was recorded every two days from the 3rd to 15th day after implantation. All mice were killed 2 weeks later, and the xenograft tumors were collected and measured tumor weight (g). All experimental protocols were approved by the Committee on the Use of Live Animals in Teaching and Research of Sichuan University. The methods were conducted in accordance with the approved guidelines.

**Tissue samples from BCC patients.** A total of 49 cases of human BCC samples were obtained from the Tumor Tissue Bank of West China Hospital. The diagnosis, pathological grade (Elston-Ellis modification of the Scarff-Bloom-Richardson Grading System) and the subtypes classification (luminal A, luminal B, Her-2-enrich cases, basal-like and normal-like) of the breast cancer for all samples were confirmed by a pathologist. To simplify the statistical analysis, we designated grades 1–2 as low grade and grade 3 as high grade. The tissues were snap-frozen in liquid nitrogen immediately after dissection and stored in liquid nitrogen until further assessment using western blot analysis. We calculated the gray value of ZNF32, LC3 II and β-actin, and then normalized the results by comparing ZNF32 or LC3 II with β-actin.

The study was approved by the local Ethical Committee on Human Experimentation of West China Hospital, Chengdu, and informed written consent was obtained from all the patients. Then, all of the collected samples were eligible for experimental purposes. The methods were conducted in accordance with the approved guidelines.

**Statistical analysis.** Statistical analyses were performed with SPSS 13.0 (SPSS, Chicago, IL, USA). One-way analysis of variance test was used to evaluate the results of the MTT assay and AO staining. Correlation analysis was conducted to examine the relationship between ZNF32 expression and LC3 II expression in breast cancer patients. Student's t test was used to analyze the differences in the ZNF32 or LC3 II expression in breast cancer samples. The equality of variances was assured by Levene's test. *P* values < 0.05 were considered statistically significant. \*Indicates that the *P* values were < 0.05 and > 0.01, whereas \*\*indicates *P* values < 0.01.

- Cannizzaro, L. A., Aronson, M. M. & Thiesen, H. J. Human zinc finger gene ZNF23 (Kox16) maps to a zinc finger gene cluster on chromosome 16q22, and ZNF32 (Kox30) to chromosome region 10q23-q24. *Hum. Genet.* **91**, 383–385 (1993).
- Li, K. *et al.* Construction of eukaryotic expression plasmid for a novel zinc finger protein gene Zfp637 and its effect on breast carcinoma cell EMT6. *Sichuan Da Xue Xue Bao Yi Xue Ban.* **40**, 575–578 (2009).
- Li, K. *et al.* A novel zinc finger protein Zfp637 behaves as a repressive regulator in myogenic cellular differentiation. *J. Cell Biochem.* **110**, 352–362 (2010).
- Sui, X. B. *et al.* p38 and JNK MAPK pathways control the balance of apoptosis and autophagy in response to chemotherapeutic agents. *Cancer Lett.* **344**, 174–179 (2013).
- Schoenfeld, T. A., McKerracher, L., Obar, R. & Vallee, R. B. MAP 1A and MAP 1B are structurally related microtubule associated proteins with distinct developmental patterns in the CNS. *J. Neurosci.* **9**, 1712–1730 (1989).
- Kabeya, Y. *et al.* LC3, a mammalian homologue of yeast Apg8p, is localized in autophagosomal membranes after processing. *EMBO J.* **19**, 5720–5728 (2000).
- Xie, R. *et al.* Microtubule-associated protein 1S (MAP1S) bridges autophagosome components with microtubules and mitochondria to affect autophagosomal biogenesis and degradation. *J. Biol. Chem.* **286**, 10367–10377 (2011).
- Tanida, I., Ueno, T. & Kominami, E. LC3 conjugation system in mammalian autophagy. *Int. J. Biochem. Cell Biol.* **36**, 2503–2518 (2004).
- Hanada, T. *et al.* The Atg12-Atg5 conjugate has a novel E3-like activity for protein lipidation in autophagy. *J. Biol. Chem.* **282**, 37298–37302 (2007).
- Twig, G. *et al.* Fission and selective fusion govern mitochondrial segregation and elimination by autophagy. *EMBO J.* **27**, 433–446 (2008).
- Narendra, D., Kane, L. A., Hauser, D. N., Fearnley, I. M. & Youle, R. J. p62/SQSTM1 is required for Parkin-induced mitochondrial clustering but not mitophagy; VDAC1 is dispensable for both. *Autophagy* **6**, 1090–1096 (2010).
- Chen, G. Y. *et al.* Graphene Oxide Triggers Toll-Like Receptors/Autophagy Responses In Vitro and Inhibits Tumor Growth In Vivo. *Adv. Healthc. Mater.* [Epub ahead of print] (2014).
- Kondo, Y., Kanzawa, T., Sawaya, R. & Kondo, S. The role of autophagy in cancer development and response to therapy. *Nat. Rev. Cancer* **5**, 726–734 (2005).
- Maycotte, P. & Thorburn, A. Autophagy and cancer therapy. *Cancer Biol. Ther.* **11**, 127–137 (2011).
- Janku, F., McConkey, D. J., Hong, D. S. & Kurzrock, R. Autophagy as a target for anticancer therapy. *Nat. Rev. Clin. Oncol.* **8**, 528–539 (2011).
- Gupta, A. *et al.* Autophagy inhibition and antimalarials promote cell death in gastrointestinal stromal tumor (GIST). *Proc. Natl. Acad. Sci. U S A* **107**, 14333–14338 (2010).
- Blanke, C. D. *et al.* Long-term results from a randomized phase II trial of standard-versus higher-dose imatinib mesylate for patients with unresectable or metastatic gastrointestinal stromal tumors expressing KIT. *J. Clin. Oncol.* **26**, 620–625 (2008).
- Blay, J. Y. *et al.* Prospective multicentric randomized phase III study of imatinib in patients with advanced gastrointestinal stromal tumors comparing interruption versus continuation of treatment beyond 1 year: The French Sarcoma Group. *J. Clin. Oncol.* **25**, 1107–1113 (2007).
- Zou, J. *et al.* Mitochondrion-associated protein LRPPRC suppresses the initiation of basal levels of autophagy via enhancing Bcl-2 stability. *Biochem. J.* **454**, 447–457 (2013).
- Levine, B., Sinha, S. & Kroemer, G. Bcl-2 family members: dual regulators of apoptosis and autophagy. *Autophagy* **4**, 600–606 (2008).
- Scarlatti, F., Maffei, R., Beau, I., Codogno, P. & Ghidoni, R. Role of non-canonical Beclin 1-independent autophagy in cell death induced by resveratrol in human breast cancer cells. *Cell Death. Differ.* **15**, 1318–1329 (2008).
- Liang, J. *et al.* The energy sensing LKB1-AMPK pathway regulates p27 kip1 phosphorylation mediating the decision to enter autophagy or apoptosis. *Nat. Cell Biol.* **9**, 218–224 (2007).
- Pattingle, S. *et al.* Bcl-2 antiapoptotic proteins inhibit Beclin1-dependent autophagy. *Cell* **122**, 927–939 (2005).
- Zarzynska, J. M. The Importance of Autophagy Regulation in breast cancer development and treatment. *Biomed Res Int.* [Epub ahead of print] (2014).
- Kimura, S., Fujita, N., Noda, T. & Yoshimori, T. Monitoring autophagy in mammalian cultured cells through the dynamics of LC3. *Methods Enzymol.* **452**, 1–12 (2009).
- D'Eletto, M. *et al.* Transglutaminase 2 is involved in autophagosomal maturation. *Autophagy* **5**, 1145–1154 (2009).
- Umeki, D. *et al.* Effects of chronic Akt/mTOR inhibition by rapamycin on mechanical overload-induced hypertrophy and myosin heavy chain transition in masseter muscle. *J. Pharmacol. Sci.* **122**, 278–288 (2013).



28. Wang, Y. *et al.* Loss of macroautophagy promotes or prevents fibroblast apoptosis depending on the death stimulus. *J Biol Chem.* **283**, 4766–4777 (2008).
29. Jia, Z. *et al.* Autophagy eliminates cytoplasmic  $\beta$ -catenin and NICD to promote the cardiac differentiation of P19CL6 cells. *Cell Signal* **26**, 2299–2305 (2014).
30. Gutierrez, E., Richardson, D. R. & Jansson, P. J. The Anti-Cancer Agent, Dp44mT, Overcomes Pro-survival Autophagy by Two Mechanisms: Persistent Induction of Autophagosome Synthesis and Impairment of Lysosomal Integrity. *J Biol Chem.* [Epub ahead of print] (2014).
31. Gurusamy, N. & Das, D. K. Autophagy, redox signaling, and ventricular remodeling. *Antioxid Redox Signal* **11**, 1975–1988 (2009).
32. Capasso, I. *et al.* Metabolic syndrome-breast cancer link varies by intrinsic molecular subtype. *Diabetol Metab Syndr.* **6**, 105 (2014).
33. Parker, J. S. *et al.* Supervised risk predictor of breast cancer based on intrinsic subtypes. *J Clin Oncol.* **27**, 1160–1167 (2009).
34. Sorlie, T. *et al.* Repeated breast tumor subtypes in independent gene expression data sets. *Proc Natl Acad Sci U S A* **100**, 8418–8423 (2003).
35. Wei, M. F. *et al.* Autophagy promotes resistance to photodynamic therapy-induced apoptosis selectively in colorectal cancer stem-like cells. *Autophagy* **10**, 1179–1192 (2014).
36. Younce, C. W. & Kolattukudy, P. E. MCP-1 causes cardiomyoblast death via autophagy resulting from ER stress caused by oxidative stress generated by inducing a novel zinc-finger protein, MCPIP. *Biochem. J.* **426**, 43–53 (2010).
37. Chen, J. W. *et al.* The response of Autophagy and Apoptosis to Oxidative Stress in Nucleus Pulposus Cells: Implications for Disc Degeneration. *Cell Physiol Biochem.* **34**, 1175–1189 (2014).
38. Jain, S. *et al.* Inhibition of autophagy increases apoptosis during re-warming after cold storage in renal tubular epithelial cells. *Transpl Int.* [Epub ahead of print] (2014).
39. Yang, Z. J., Chee, C. E., Huang, S. & Sinicrope, F. A. The role of autophagy in cancer: therapeutic implications. *Mol Cancer Ther.* **10**, 1533–1541 (2011).
40. Kenific, C. M., Thorburn, A. & Debnath, J. Autophagy and metastasis: another double-edged sword. *Curr Opin Cell Biol.* **22**, 241–245 (2010).
41. Eskelinen, E. L. The dual role of autophagy in cancer. *Curr Opin Pharmacol.* **11**, 294–300 (2011).
42. Palumbo, S. & Comincini, S. Autophagy and ionizing radiation in tumors: the “survive or not survive” dilemma. *J Cell Physiol.* **228**, 1–8 (2013).
43. Wei, Y. *et al.* Establishment of a monoclonal antibody against a peptide of the novel zinc finger protein ZNF32 proved to be specific and sensitive for immunological measurements. *Med. Sci. Monit.* **18**, 167–173 (2012).

## Acknowledgments

This study was supported by the grants (31070675) from National Natural Science Foundation of China and by Sichuan Province foundation (2014SZ0020) from Science and Technology Department of Sichuan Province. This work was also supported by the grants (81401979) from National Natural Science Foundation of China and by Project fund (2014M552367) from China Postdoctoral Science Foundation.

## Author contributions

Y.L. carried out the research and drafted the manuscript. L.Z. revised the manuscript. K.L. and J.L. helped to feed and prepare the mice. R.X. and Y.W. kindly offered valuable suggestions about the experiment design. J.Z. provided some cell culture. H.L. and Y.X. provided human BCC samples. Y.W. and J.G. provided pSG5-ZNF32 over-expression plasmid and transfection. P.L. designed the experiments, analyzed the results and revised the manuscript. All authors reviewed the manuscript.

## Additional information

**Supplementary information** accompanies this paper at <http://www.nature.com/scientificreports>

**Competing financial interests:** The authors declare no competing financial interests.

**How to cite this article:** Li, Y. *et al.* ZNF32 inhibits autophagy through the mTOR pathway and protects MCF-7 cells from stimulus-induced cell death. *Sci. Rep.* **5**, 9288; DOI:10.1038/srep09288 (2015).



This work is licensed under a Creative Commons Attribution 4.0 International License. The images or other third party material in this article are included in the article's Creative Commons license, unless indicated otherwise in the credit line; if the material is not included under the Creative Commons license, users will need to obtain permission from the license holder in order to reproduce the material. To view a copy of this license, visit <http://creativecommons.org/licenses/by/4.0/>